JOURNAL OF MATERIALS SCIENCE **34** (1999) 5243–5255

Experimental and theoretical studies of palygorskite clays

M. E. FERNÁNDEZ*, J. A. ASCENCIO*, D. MENDOZA-ANAYA*,
V. RODRÍGUEZ LUGO*, M. JOSÉ-YACAMÁN*‡
Instituto Nacional de Investigaciones Nucleares, Amsterdam 46-202, Hipódromo Condesa, 06100 México, D.F. MEXICO
‡*Instituto de Física—UNAM, Apartado Postal 20-364, 01000 México, D.F. MEXICO*
E-mail: ascencio@nuclear.inin.mx

We have studied the structure and properties of palygorskite clays. A structure analysis was performed using two different models to reproduce the monoclinic and orthorhombic lattices, using the atomic positions and cell parameters of palygorskite structure suggested by several authors, we simulated structures using Molecular Dynamics and Quantum Mechanics. Modifications on the structure and elemental atom changes were made to obtain more stable configurations. X-ray diffraction patterns and high resolution electron microscopy images from simulated structures were compared with experimental results. It could be observed that orthorhombic model shows a better fitting than monoclinic models. These results might help to understand many of the properties of archaeological pigments, such as, Maya Blue, in which palygorskite clay was the main component. © *1999 Kluwer Academic Publishers*

1. Introduction

Palygorskites are important clay minerals for many applications of modern materials science. Palygorskite belongs to the family of phyllosilicates with a number of important properties, such as sorptive, rheological and catalytic properties [1–5]. These clays have been industrially used to absorb oil, water, chemicals and even toxic wastes. It is also well known that the silanol groups of palygorskite can react with organic reagents to produce covalent bonds that strongly attach the organic substances to the clay.

One of the uses of this clay, which is important for historical and cultural reasons, is its use by American ancient cultures. During Pre-Colombian mesoamerican period, this clay was widely used to manufacture an important dye, called Maya blue, which is a combination of palygorskite, indigo and metallic particles [6–9]. Indeed new studies indicate that palygorskite was used in other colorants such as yellow, green and red [9].

In these notes, we report the results on the study of the simulated structure of palygorskite using molecular dynamics and quantum mechanics. Finally, we are including a comparison between the simulated and experimental results obtained by X-ray Diffraction, Transmission Electron Microscopy and related techniques.

2. Experimental methods

Experimental studies were made using palygorskite samples from mines of the Yucatan peninsula. These samples were crushed and mounted for the analysis in the proper holder. X-ray diffraction studies were performed using a SIEMENS D5000 diffractometer, operated to 30 keV and 25 mA. A scanning from 2° to 70° with steps of 0.1° were made. Transmission Electron Microscopy (TEM) was performed on JEOL 2010 Microscopy with a spherical aberration coefficient, $C_s \approx 0.5$ mm and a point resolution of ~ 1.94 Å at the Instituto Nacional de Investigaciones Nucleares, and a JEOL 4000-EX microscope fitted with a Gatan TV Camera with $C_s \approx 1.0$ mm and a resolution point of 1.7 Å at the Instituto de Física, UNAM.

Calculations of the structure were made using a Molecular Dynamics approximation, for the largest structures and the crystal packing refinement, employing a Force-field. Also, an *ab-initio* quantum mechanic method was used to calculate the local geometry optimization considering the Density Functional Theory (DFT) in the Local Density Approximation (LDA) using the gradient corrected LDA developed by Perdew and Wang (GGA).

High Resolution simulated images were obtained at the Scherzer condition for the Jeol 4000-EX using the Cerius^2 software from Molecular Simulation Inc. These calculations were run over a Solid Impact Work Station with a R10000 processor of Silicon Graphics Inc.

3. Models of palygorskite

The palygorskite mineral constitute a particular group within clays, its structure contains continuos planes of tetrahedral basal oxygen atoms approximately 6.5 Å apart [10–12]. The apical oxygens are up and down alternately pointing in reference to the basal oxygens planes into a pattern, in such way that the tetrahedra are pointing in the same direction form tetrahedral ribbons, which are parallel extended to X-axis. The ribbons width is average along Y of two linked pyroxene-like single chains. Ribbons with apices pointing up are linked vertically to ribbons with apices pointing down forming octahedral coordination groups around Mg and Al. The linked ribbons thus form a 2:1 layer that is continuos along X but of limited lateral extent along Y. That is, the tetrahedral sheet is continuos across ribbons, but with apices pointing in different directions to adjacent ribbons. Oxygen atoms in the octahedra at the edge of the ribbons are coordinated to cations on the ribbon side only, and coordination and charge balance are completed along the channel by protons, coordinated water and a small of exchangeable cations. The atomic positions produce a structure with present channels of 3.7 × 6.0 Å of cross section, parallel extend to the bands. Water molecules run through these channels are susceptible to get lost by dehydration under relatively low temperatures and can even be replaced by organic similar dimensions molecules. Fig. 1 shows the palygorskite appearance of a superlattice with a standard model in the [0 0 1] direction.

Palygorskite can be found in a wide variety of environments. It has been identified in oils, continental and marshy sediments in low deep seas, saline and carbonic depots. Some data show that it can be formed by hydrothermal action in amphiboles and piroxenes, or by the alteration of volcanic ashes and basalt. Studies realized on this clay [10–12] have established the most likely composition is $(Mg,Al)_4Si_8(O,OH,H_2O)_{24}$, being a combination of two crystalline forms: orthorhombic and monoclinic.

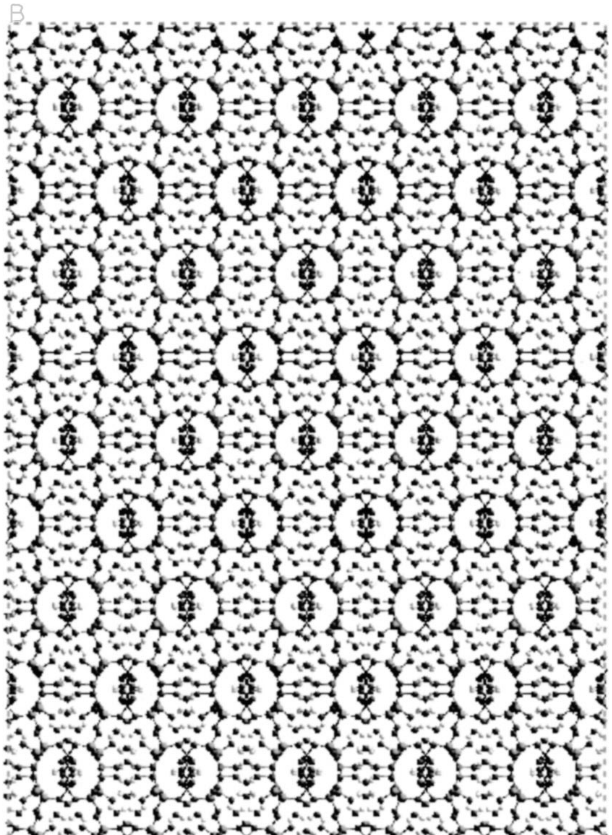

Figure 1 Standard model of palygorskite clay oriented in [0 0 1] to illustrate the channels.

TABLE I Monoclinic System. Atomic Positions (Asymmetrical Unity)

Atom	x/a	y/b	z/c	Occupance
Si1	0.197(1)	0.080(1)	0.089(4)	1.00
Si2	0.215(1)	0.166(1)	0.591(4)	1.00
Mg2	0.0	0.084(2)	0.5	1.00
Mg3	0.0	0.193(2)	0.0	1.00
Oh1	0.088(3)	0.0	0.52(1)	1.00
O1	0.084(2)	0.093(2)	0.154(5)	1.00
O2	0.097(2)	0.170(1)	0.634(6)	1.00
W1	0.075(2)	0.296(2)	−0.050(7)	1.00
O3	0.242(3)	0.0	0.023(9)	1.00
O4	0.25	0.25	0.5	1.00
O5	0.252(2)	0.105(2)	0.400(5)	1.00
O6	0.250(2)	0.127(2)	0.889(5)	1.00
ZW1	0.0	0.344(3)	0.5	1.00
ZW2	0.0	0.427(3)	0.0	1.00

TABLE II Orthorhombic System. Atomic Positions (Asymmetrical Unity)

Atom	x/a	y/b	z/c	Occupance
Si1	0.2669(8)	0.0913(4)	0.799(2)	1.00
Si2	0.1948(6)	0.1677(5)	0.322(2)	1.00
Mg2	0.0	0.072(2)	0.5	0.37(3)
Mg3	0.0	0.173(1)	0.0	1.00
Oh1	0.070(2)	0.0	0.220(5)	1.00
O1b	0.034(1)	0.0798(8)	0.788(3)	1.00
O2	0.0694(8)	0.172(1)	0.372(3)	1.00
W1	0.089(1)	0.225(1)	0.372(3)	1.00
O3	0.262(2)	0.0	−0.146(4)	1.00
O4	0.25	0.25	0.385(5)	1.00
O5	0.270(1)	0.1162(9)	0.504(2)	1.00
O6	0.233(2)	0.126(1)	0.068(2)	1.00
O7	0.360(5)	0.153(4)	0.86(2)	0.24(2)
ZW2	0.0	0.441(2)	0.0	1.21(6)
ZW3	0.0	0.359(3)	0.5	1.07(6)
ZW4	0.405(3)	0.031(3)	0.243(8)	0.53(3)
Mg4	0.249(3)	0.0	0.250(9)	0.18(3)

To analyze the data obtained in this work, we test different models; three monoclinic models and one orthorhombic. These structures can be described as follows; the monoclinic system has cell parameters $a = 13.274$ Å, $b = 17.868$ Å, $c = 5.279$ Å, $\beta = 107.38^\circ$; the atomic positions (asymmetrical unit) are shown in Table I. Using the cell parameters and the atomic positions, we tested different monoclinic configurations. Fig. 2 shows the first studied model, where it is possible to identify a centred local structure formed by atoms of magnesium and silicon joined by oxygen, and several H_2O molecules between these structures. A detailed observation in this structure can show just three oxygen atoms around each silicon atom.

According to E. Besoain [5] Si atoms should yield tetrahedron and Mg octahedral sheets, but these shapes could not be observed in the model, this means there are no enough oxygen atoms to make four triangles with similar dimension and equidistant to a central silicon atom. To solve this problem we added an oxygen atom to basal oxygens, which generates the tetrahedron sheets. On the other hand, several authors [10–12] have suggested that the stability of palygorskite structure appears when it has a central atom, therefore, if we add a Mg or Al atom to the model, it becomes a more

TABLE III Analysis of reports[a] and simulated[b] results

	Report[a]			Models			Model 4	
hkl	*d*(A)	Intensity	*d*(A) M1 = M2 = M4	Intensity M1	Intensity M2	Intensity M3	*d*(A)	Intensity M4
110	10.5	100	10.3484	100	100	100	10.3805	64.83
200	6.44	60	6.347	38.85	77.89	6.7	6.3815	23.56
130	5.42	50	5.392	0	0.02	5.14	5.3908	64.83
040	4.49	80	4.467	28.06	48.81	3.98	4.4605	41.58
310	4.189	30	4.1175	10.38	8	0	4.1383	4.71
240	3.69	50	3.653	2.25	10.34	7.99	3.6559	35.74
330	3.5	30	3.4399	0.9	0.88	0.71	3.4366	10.16
150	3.5	30	3.4495	0.79	0.56	2.59	3.4602	3.53
400	3.23	100	3.1735	38.85	54.86	20.04	3.1907	100
420	3.03	10	2.9904	0.29	0.05	0.98	3.0044	9.53
440	2.61	80	2.5871	4.4	9.22	0.4	2.5951	44.13
510	2.55	30	2.5136	0.02	0	0.63	2.5269	0
530	2.38	30	2.3355	0.91	0.77	0.04	2.3457	6.62
600	2.15	50	2.1157	6.37	10.08	1.46	2.1272	8.56
390	1.82	10						
800	1.62	10						
680	1.56	30						
120	1.5	50						

[a] Besoain, Eduardo. Minerología. Instituto Interamericano de Cooperación para la agricultura, San José de Costa Rica.

[b] Simulated date in Cerius^2.

M1 = Model 1. Crystalline monoclynical system.

M2 = Model 2. Crystalline monoclynical system with an atom plus for formed tetrahedro.

M3 = Model 3. Crystalline monoclynical system. Based in the model 2 with an atom of Mg o Al in the center.

M4 = Model 4. Crystalline orthorhombic system.

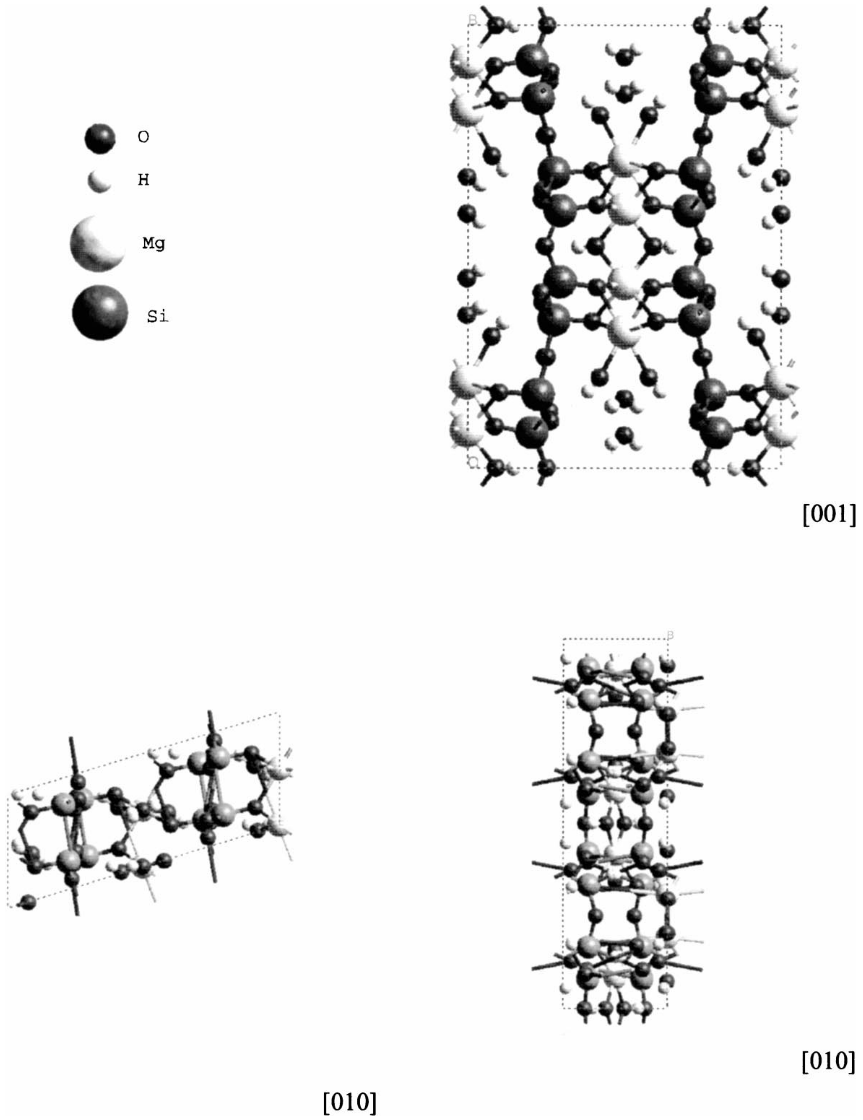

Figure 2 Monoclinic structure reported for palygorskite [1].

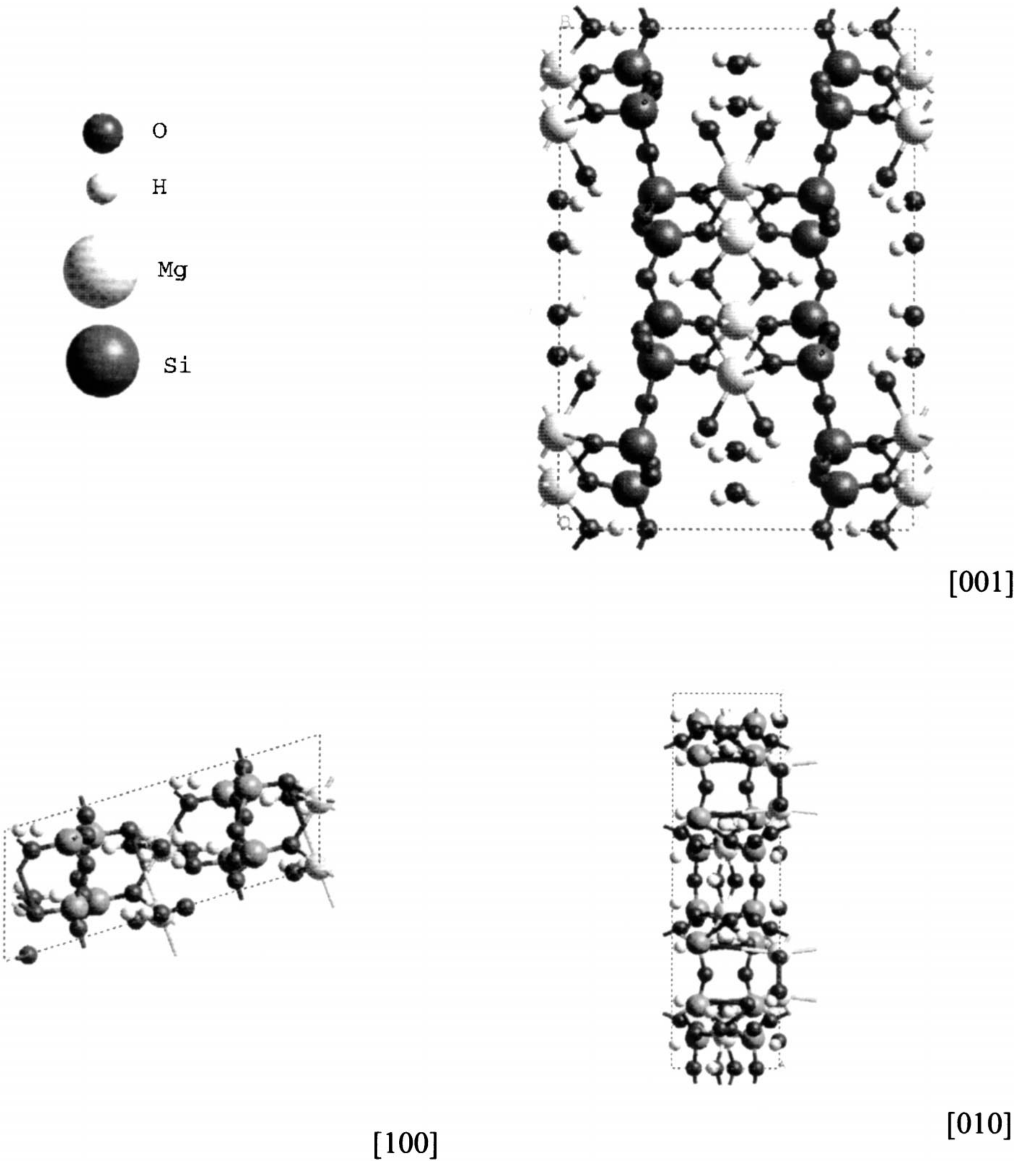

Figure 3 Monoclinic structure with magnesium central atom and extra oxygen atoms to complete the suggested tetrahedral shapes.

stable configuration when molecular simulation techniques are used and octahedral sheets are generated. This model is shown in Fig. 3, the difference with the previous model are observed in the [0 0 1] orientation, where there is a central magnesium atom, and in the [0 1 0] orientation the extra oxygen atoms are localized in left and right lattice edges.

In the orthorhombic system, we have cell parameters $a = 12.763$ Å, $b = 17.842$ Å, $c = 5.241$ Å; space group: Pbmn; the atomic position atoms (asymmetric unit) are shown in Table II.

We generated a structure of palygorskite using an energy minimization procedure. Variations in positions or distances were present, this model is shown in Fig. 4. In the [0 0 1] orientation is shown that the central solid shape, composed by the magnesium, silicon and oxygen atoms, is wider than the monoclinic structure and the channels will be smaller.

4. X-ray diffraction spectra of palygorskite

Calculations shown that the proposed structures of palygorskite have energetic stability. To refine the model, X-ray diffraction patterns were obtained for each structure (Fig. 5a, b and c), which were compared with the experimental results.

A comparative analysis shows to monoclinic models corresponds to the palygorskite structure, due mainly that the interplanar distances are similar to experimental results, however some variations in the peak intensities were observed. The orthorhombic model, also shows some changes with absorption intensities but, it can be appreciated a better approximation with experimental results than with monoclinic models, as shown in Table III in which the atomic planes (hkl), interplanar distances (d) and absorption intensities (I) corresponding to palygorskite sample and simulated structures of monoclinic and orthorhombic lattices are compared.

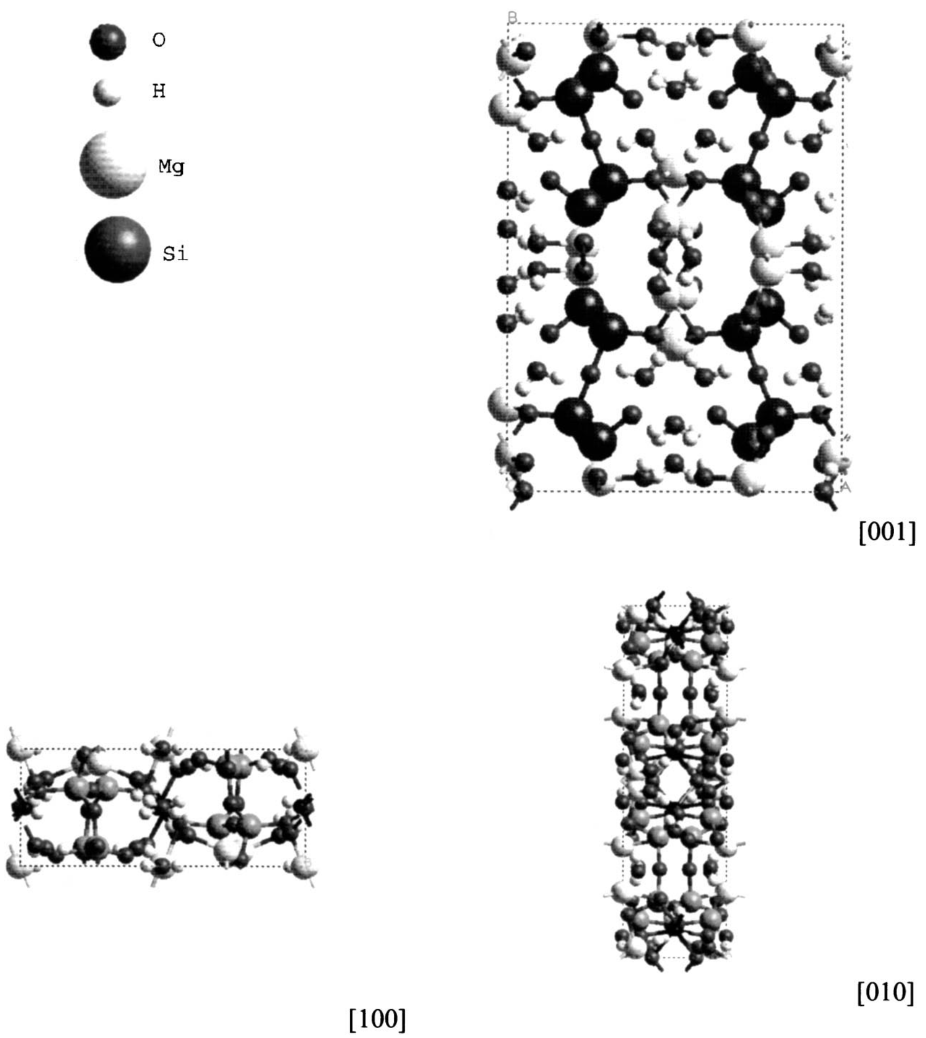

Figure 4 Orthorhombic structure reported for palygorskite [1].

TABLE IV Orthorhombic System. With a substitution of one mg per one Fe and two mg per teo Al atoms. Atomic Positions (Asymmetrical Unity)

Atom	x/a	y/b	z/c	Occupance
H	0.0544	0.4678	−0.0010	1.00
O	0.0633	0.1657	0.3652	1.00
H	0.0315	−0.0464	0.3402	1.00
O	0.0000	0.4403	0.0000	1.00
Al	0.0052	0.1847	−0.0048	1.00
O	0.2591	0.0934	0.5295	1.00
O	0.0000	0.3578	0.5001	1.00
O	0.0514	0.0000	0.2860	1.00
Al	0.2767	0.0260	0.1269	1.00
H	0.0597	0.3721	0.5510	1.00
H	0.4102	0.0550	0.3988	1.00
Fe	−0.0179	0.0770	0.4902	1.00
O	0.2717	−0.0297	−0.1679	1.00
Si	0.2699	0.1062	0.8481	1.00
O	0.2500	0.2500	0.3553	1.00
O	0.0893	0.2560	0.8493	1.00
H	0.0485	0.2179	0.8748	1.00
H	−0.0469	0.3878	0.5516	1.00
H	0.1518	0.2422	0.8598	1.00
O	0.2261	0.1210	0.0555	1.00
SI	0.1980	0.1586	0.3408	1.00
H	−0.0544	0.4678	0.0010	1.00
O	0.4108	0.0295	0.2616	1.00
O	0.0537	0.0610	0.8241	1.00
O	0.3726	0.1633	0.9094	1.00

5. Refinement of the model for the palygorskite structure

In accordance with the X-ray diffraction analysis for each one of the proposed structures, some atoms that produced strong variations in the peak intensities were tested and exchanged respectively.

The elements substitution in the monoclinic model was performed under the following independent sequences:

- A first substitution of all Mg atoms per Al was made.
- A second modified model was obtained exchanging one Mg atom per Ca and two Mg atoms per two Al.
- A last substitution of one Mg atom per Fe and two Mg atoms per two Al generated the last monoclinic model.

The obtained models for each operation were studied by X-ray diffraction analysis, however the results show that the model with a central atom and with Al atoms instead of Mg, intensities are increased as required, however, a close analysis indicates that the model with a substitution of a Mg atom per Fe and two Mg per two Al yields a more close fitting with the experimental data. Therefore, for the monoclinic symmetry lattice case, the last model generates enough conditions to consider it is the optimum (Fig. 6). The resulting chemical composition was $Al_4Fe_2Si_8(O,OH,H_2O)_{36}$.

Similarly an elements substitution in the orthorhombic model was performed, considering the differences between the theoretical and experimental analytical data, under the following self-reliant procedures:

- First model was made substituting all Mg atoms per Al.
- A second model is obtained exchanging one Mg atom per one Ca and two Mg per two Al.

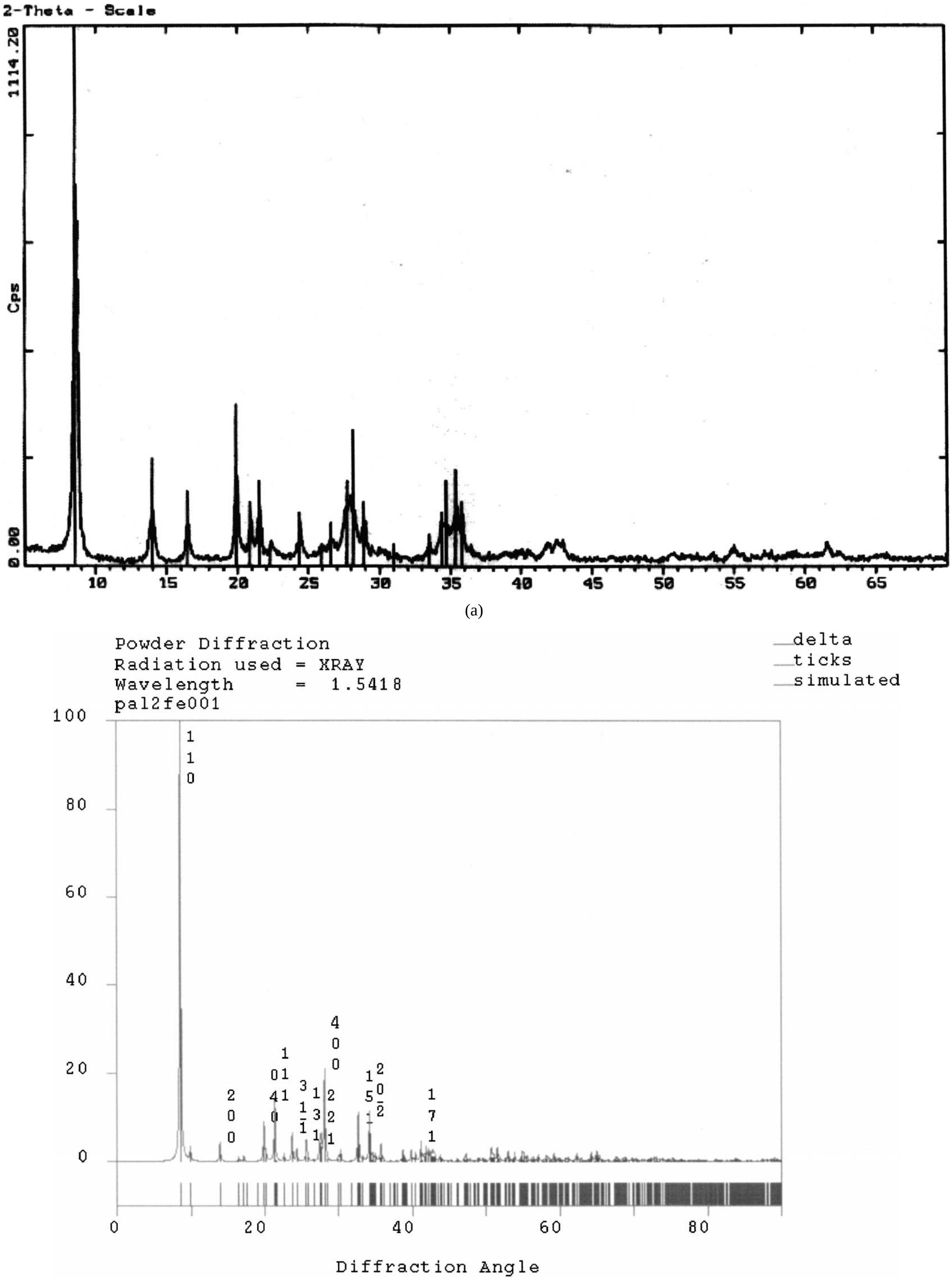

Figure 5 X-ray diffraction. (a) Experimental and (b) monoclinic and (c) orthorhombic simulate structure. (*Continued*.)

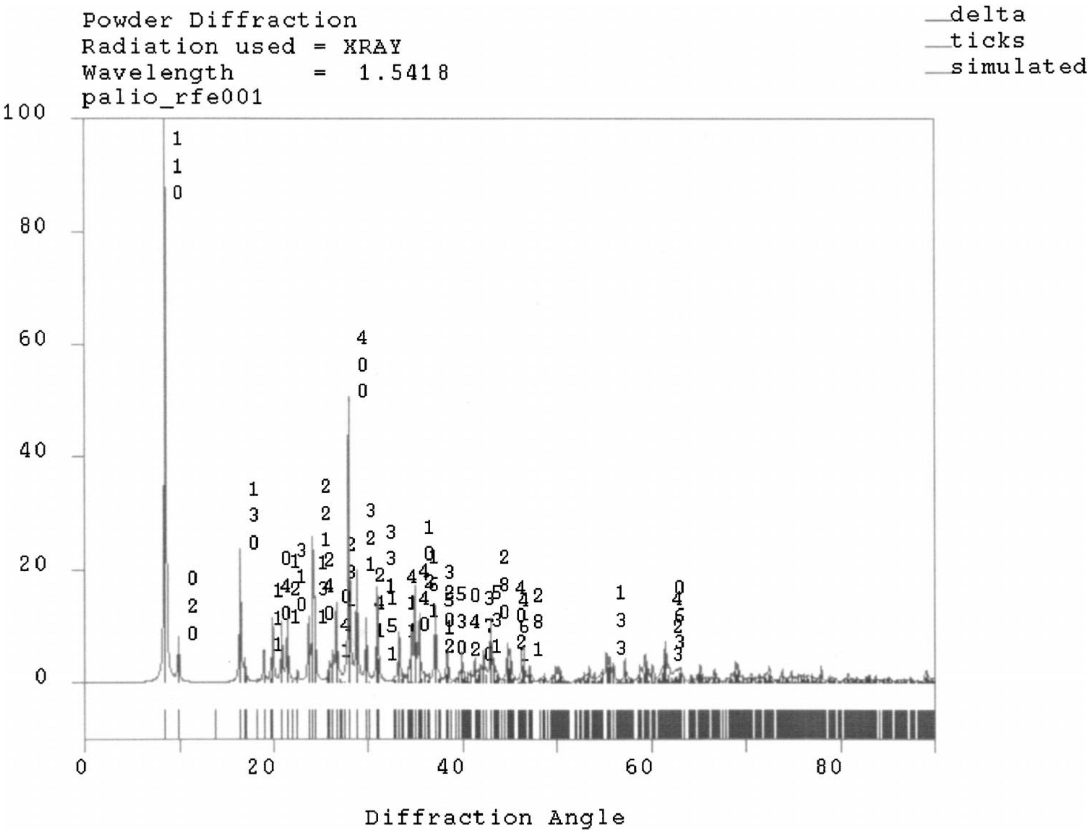

(c)

Figure 5 (*Continued*.)

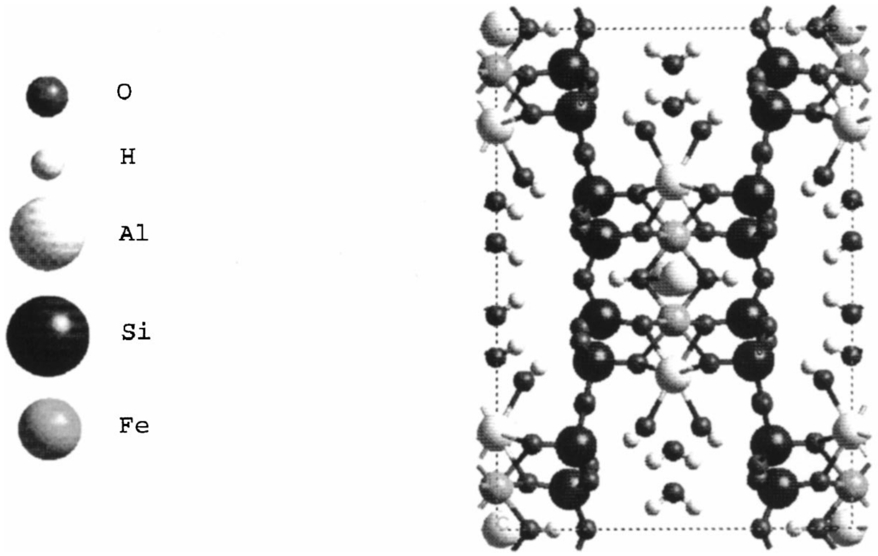

Figure 6 Monoclinic model with central atom and the substitution of a Mg atom by Fe and two Mg per two Al. [0 0 1] orientation.

- The third considered substitution implies the change of one Mg atom per one Fe and two Mg per two Al.

X-ray diffraction analysis, over the obtained models, indicates that the model with a substitution of a Mg atom per one Fe and two Mg per two Al yields a more approximated fitting with the experimental data (Fig. 7). The resulting chemical composition was $Fe_4Al_8Si_8(O,OH,H_2O)_{40}$ and the atomic positions of the asymmetrical unit are presented in Table IV. Therefore this orthorhombic model shows an excellent fitting with experimental X-ray diffraction results and due its stability we should consider it as the most representing calculated model for the palygorskite structure.

6. Calculation of external morphology of the palygorskite crystal

Considering that the knowledge of shape and aspect ratio is fundamental to understanding packing and flow problems as the possible phenomena of indigo molecules insertion in the palygorskite structure to generate the Maya Blue pigment, a simulation about the possible macroscopic morphology is made through

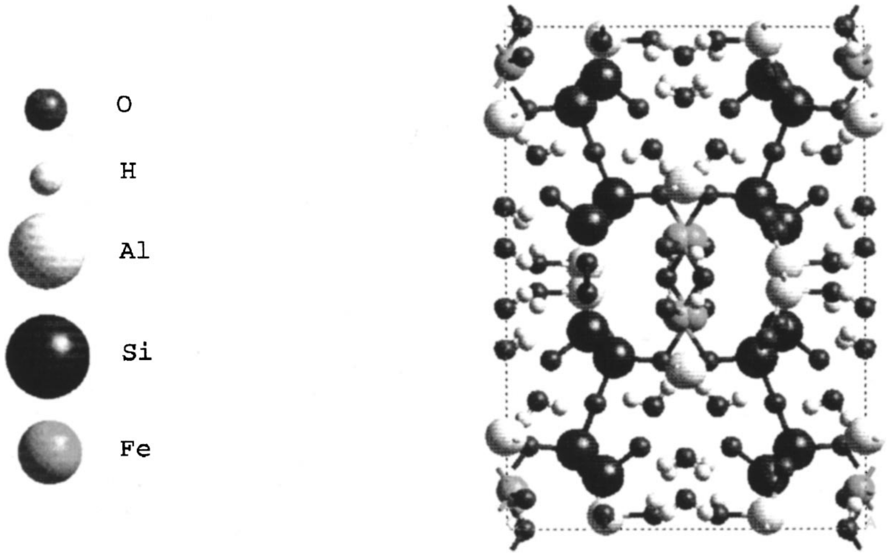

Figure 7 Orthorhombic model with the substitution of a Mg atom per one Fe and two Mg per Two Al. [0 0 1] orientation.

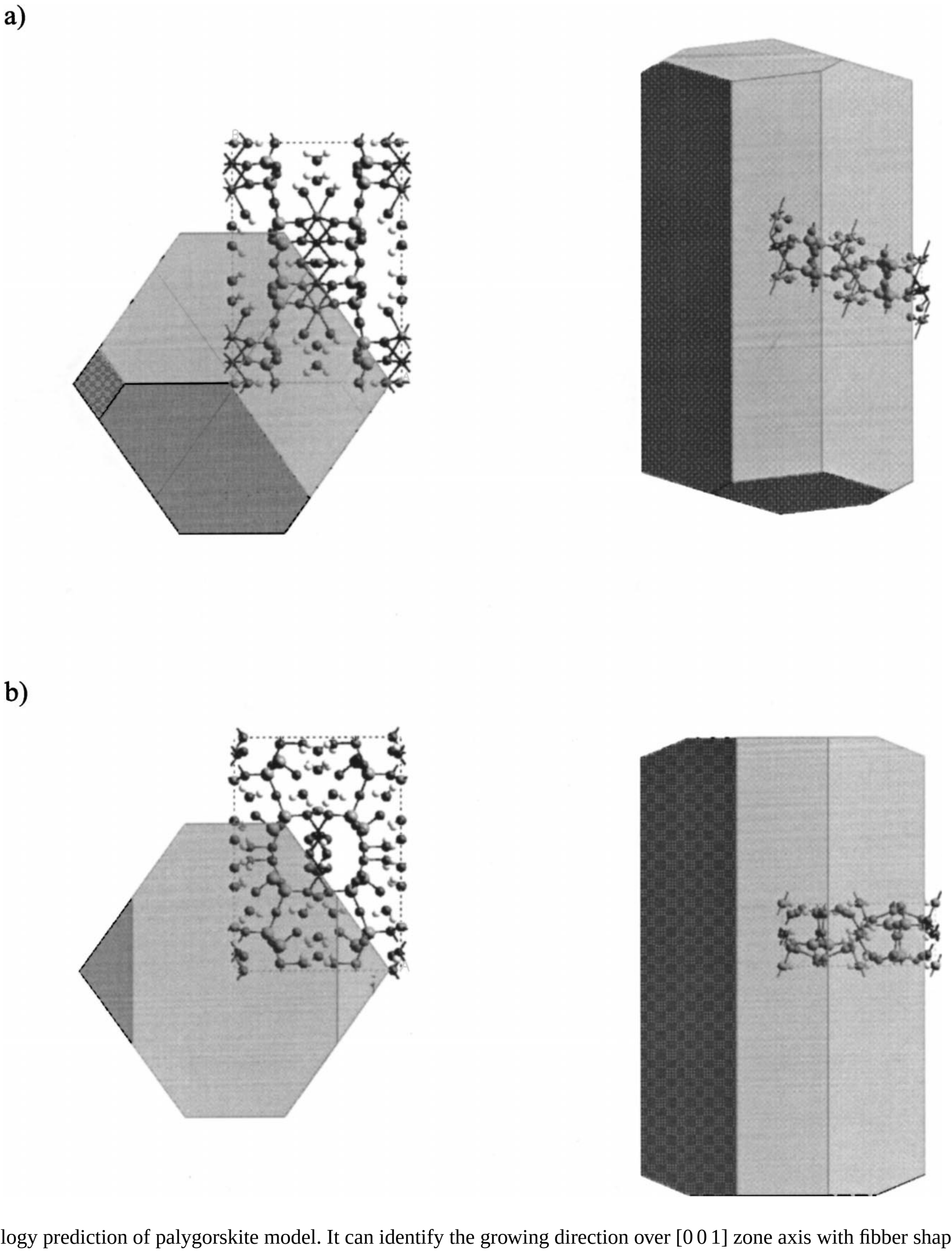

Figure 8 Morphology prediction of palygorskite model. It can identify the growing direction over [0 0 1] zone axis with fibber shape (a) monoclinic system (b) orthorhombic system.

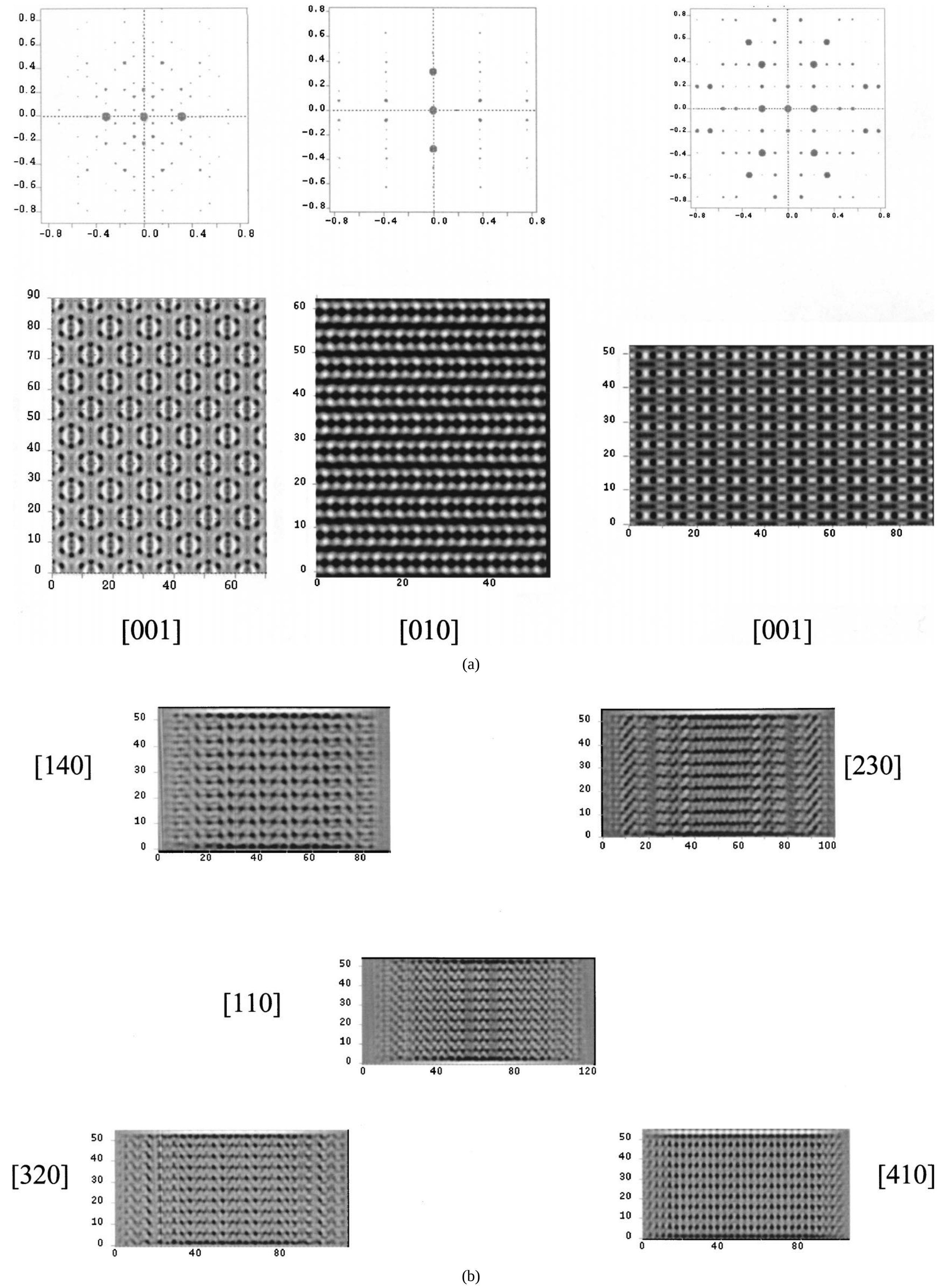

(a)

(b)

Figure 9 HREM simulate image of palygorskite model and their diffraction patterns in (a) main directions and (b) other important orientations.

fundamental characteristics of the postulated unit cell and using the Bravais-Friedel-Donnay-Harker method.

This method consists in a geometrical calculation employing information of the crystalline structure, as the crystal lattice and any translational symmetry operator present, to generate a list of possible growth faces and their relative growth rates. This calculus are also supported on the attachment energy, which is defined as the energy released on the attachment of growth slice to a growing crystal surface. The obtained result define

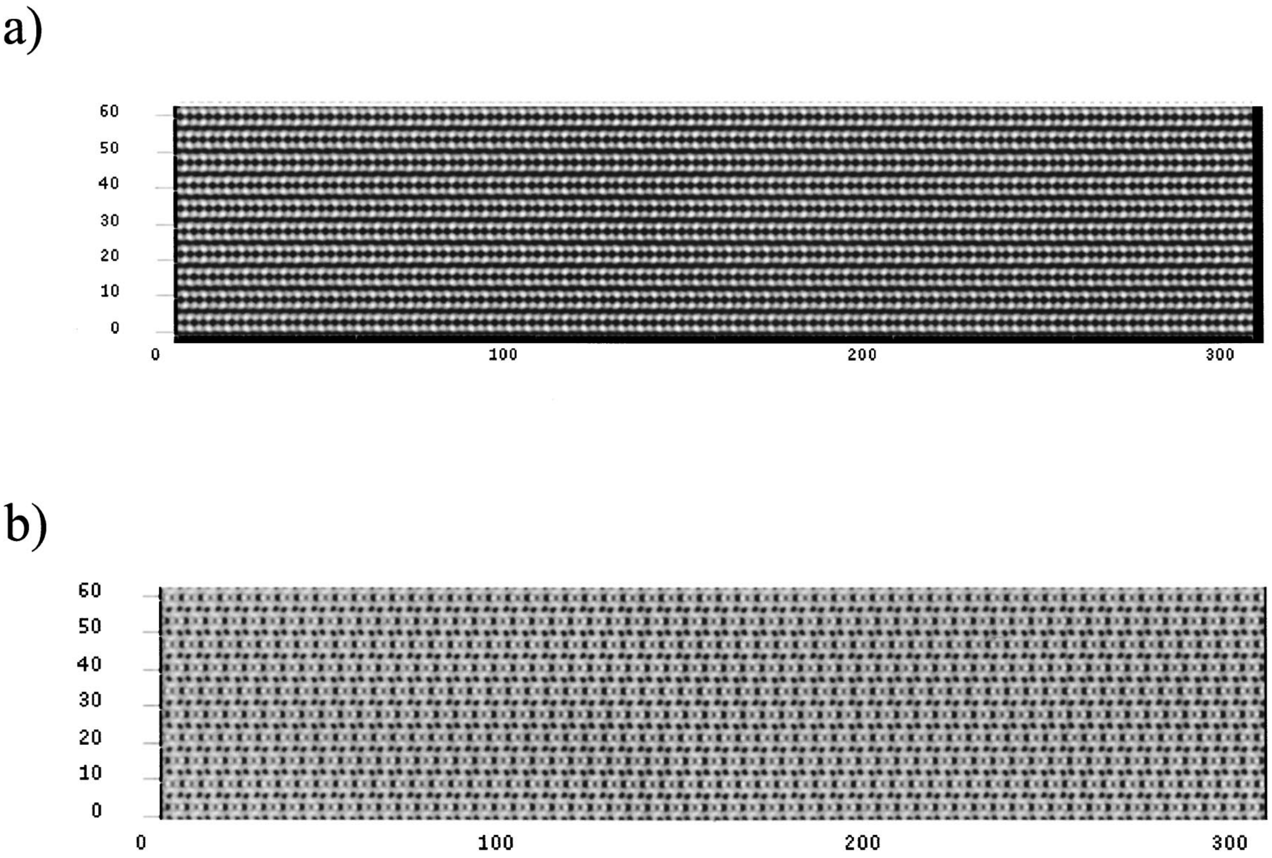

Figure 10 HREM simulate image in direction [0 1 0], where the contrast of lines is best shown and it is possible to compare favourably with the experimental images. Images calculated with a defocus of (a) −405 Å and (b) −702 Å.

a configuration in a fibber shape with specific and preferential direction to the pores growth identified in the material, it means, on [0 0 1] direction.

In the Fig. 8, [0 0 1] and [0 1 0] orientation are shown for each resulting palygorskite model to find the specific characteristics, which have been found in previous morphological studies of palygorskite. This calculated shape is similar in both crystal lattice cases, monoclinic and orthorhombic, with a small difference of the longitudinal faces area between them, and a quite different (001) face, but growing over the same [0 0 1] direction.

7. HREM images of palygorskite

7.1. Calculated images

Using a calculated model, the orthorhombic model with a substitution of a Mg atom per one Fe and two Mg per two Al, as the best configuration, we have obtained the corresponding HREM images having different orientations, this with the purpose of making a comparison between experimental and theoretical results.

The Cerius software of Molecular Simulation Inc. was employed to calculate the high resolution images and diffraction patterns of palygorskite in a number of crystallographic directions. In order to do it, we made a superlattice from the primary cell and calculating by the multi-slice method the projected potential considering the characteristic wave function to the electron beam has changes just in a phase term in relation to the original wave function, calculating next the diffraction pattern. After that, CTF (Contrast Transfer Function) was used to obtain the HREM images. Calculations were made using electron energy of 400 keV ($\lambda = 0.01644$), $C_s = 1$ mm and a defocus of −405 Å.

Fig. 9a shows the main orientations, these results are calculated for the case of optimum Scherzer defocus, while Fig. 9b shows other possible visible orientation, where the fibber contrast are observed. In order to produce the observed contrast of lines inside the fibber shapes of the experimental results, calculations of a HREM image of a bigger area in the fibber are presented in Fig. 10; these images are shown in the optimum Scherzer defocus and the second maximum of the contrast (−702 Å).

7.2. Experimental images

A typical low magnification of palygorskite structure obtained by TEM is shown in Fig. 11. It can be observed fibber shapes with thickness from 8 to 30 nm and even 1.0 μm length. These configurations are compared with the morphology obtained by simulation; even more, it is possible to find the growing up direction.

Higher magnification of a palygorskite fibber obtained by HREM is shown in Fig. 12a. The contrast of lines inside the fibber can be observed, also it is possible to observe the orientation near to [0 0 1]. It seems to be a good fitting of the images in the some directions. Particularly, the fibber images in Fig. 10 are well reproduced by calculations.

With help of image processing a better image is obtained in the Fig. 12b, where the amplification is fixed over a local area, the evidences of contrast of lines, and

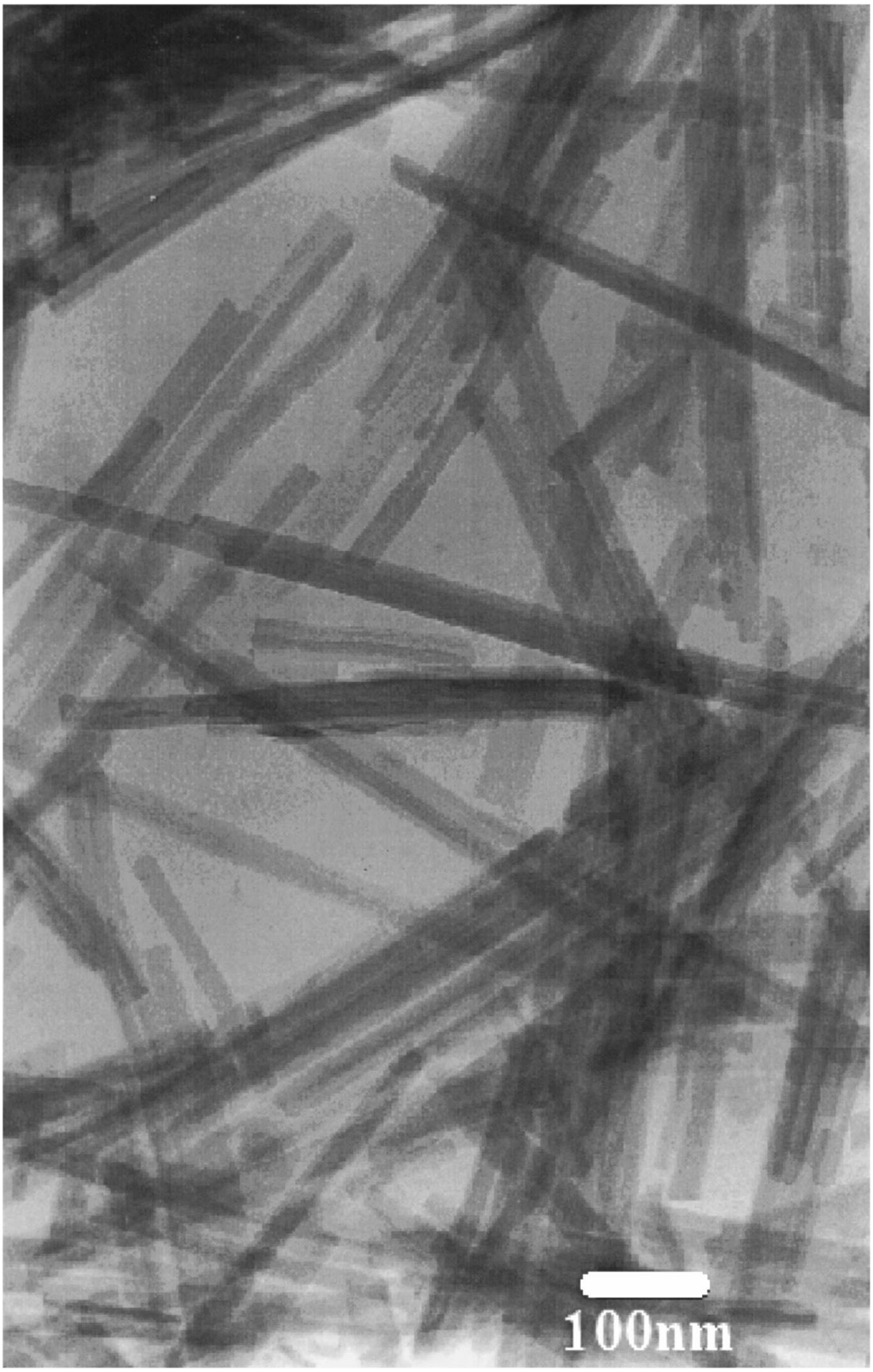

Figure 11 Micrograph obtained by TEM of a palygorskite sample (60000X magnification). It is observed fibber structure with thickness from 30 to 60 nm.

the structure of the material have the same spacing and dotting contrast than Fig. 8, where we may say that this contrast is produced by superposition of atoms when the palygorskite structure is observed in the [0 1 0] orientation and linear spacing of ∼0.3 nm. In order to get a full characterization, the Fast Fourier Transform (FFT) is applied over the HREM image and compared with the simulated diffraction pattern and evidently they have the same symmetry and this image is defined as [0 1 0] face of a palygorskite fibber. In fact the HREM with its corresponding FFT can serve to corroborate the palygorskite model and the theoretical prediction of structure and composition.

The possibility to observe the channel configuration in experimental studies is no easy, because the image corresponds to the growing direction and it would mean to have the fibber parallel to the electron beam direction.

A close analysis over the dotting contrast and the structure of the model associated with the experimental and theoretical images indicates that the silicon atoms

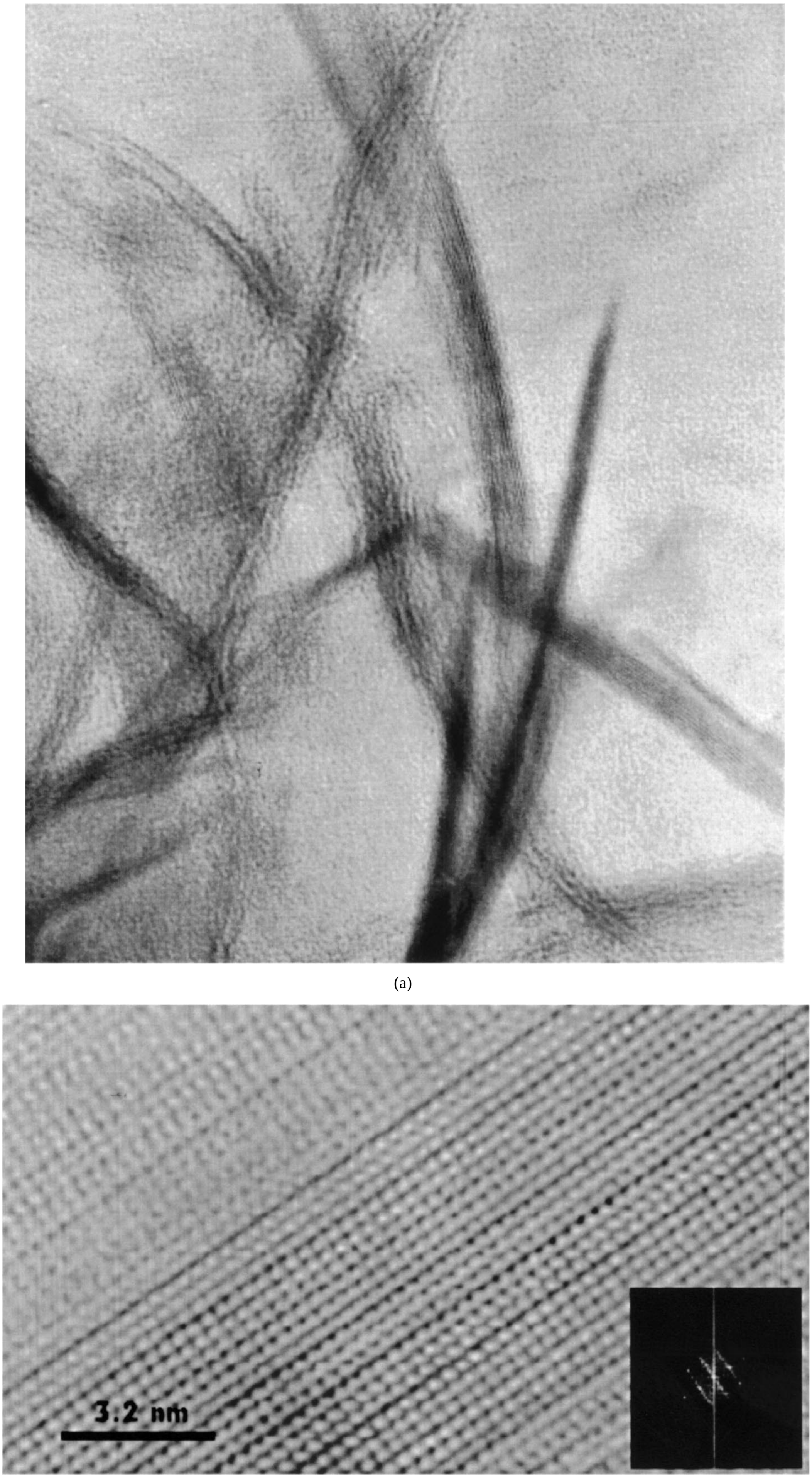

(a)

(b)

Figure 12 HREM image of palygorskite sample. (a) A big area photography shows the contrast of lines over the fibbers. (b) Image processing of HREM image with its FFT corresponding.

as the main source to produce the HREM contrast, therefore the configuration of spacing and symmetry observed in the images are related mainly with the silicon atoms arrangement.

8. Conclusions

We simulated crystalline structures of palygorskite; with two models, a monoclinic, an orthorhombic.

The monoclinic resulting model must have a central atom to show a better energetic stability, its composition is made by substituting Mg per Al and Fe atoms, also one oxygen atom is added around the silicon atoms to form octahedral sheets.

X-ray diffraction analysis shows that, the orthorhombic model has the best fitting with the experimental results. The orthorhombic lattice, where Mg atoms were substituted per Al and Fe atoms and applying an energy minimization, generates similar peaks and intensities in the X-ray analysis for simulated and experimental patterns of palygorskite samples.

Moreover this model generates a growing morphology over [0 0 1] axis, where the porous configuration is observed, also the lines formed by dots in HREM and X-ray diffraction patterns are found similar to experimental evidences on palygorskite samples.

Acknowledgement

The authors are indebted to Ricardo Reglero, Gustavo Silva, Mario Perez, Tomás Santamaría, Samuel Tehuacanero and Luis Rendon for technical assistance and CONACYT for support within the projects "Coloides Cuánticos" (G0032-A) and "Materiales Nanoestructurados" (3795P-A).

References

1. E. GALAN, *Clays Minerals* **31** (1966) 443.
2. W. F. BRADLEY, *Am. Miner.* **25** (1940) 405.
3. J. CORNEJO and M. C. HERMOSIN, *Clay Miner.* **23** (1988) 391.
4. M. N. FENÁNDEZ-HENANDÉZ and E. RUÍZ, *ibid.* **13** (1978) 375.
5. J. M. GALAN and C. SÁNCHEZ, *Appl. Clay Sci.* **9** (1994) 293.
6. VAN OLPHEN, *Science* **154** (1966) 645.
7. GETTENS, *American Antiquity* **27(4)** (1962).
8. M. JOSE YACAMÁN, L. RENDON, J. ARENAS and MARI CARMEN-SERRA PUCHE, *Science* **273** (1996) 223.
9. D. MENDOZA-ANAYA, V. RODRIGUEZ-LUGO, G. MARTINEZ-CORNEJO, A. CAMACHO-BRAGADO and M. JOSÉ-YACAMÁN, "A microstructural Study of Totonaca paintings from the Archaeological Site of Tajin," to be published.
10. ARTIOLI and E. GALLI, *Materials Science Forum* **166-169** (1994) 647.
11. G. W. BRADLEY and G. BROWN, "Crystal Structure of Clay Minerals and their X-ray Identification," edited by Mineralogical Society, 41 Queen's Gate, London SW7 5HR, 1980.
12. E. BESOAIN, Mineralogía de arcillas de Suelos. Instituto Interamericano de Cooperación para la Agricultura (San José de Costa Rica, 1995).

Received 19 August
and accepted 23 December 1998